東北大学機関リポジトリ
TOUR
Tohoku University Repository

# Synchrotron-Radiation-Induced Decomposition of Thin Native Oxide Films on Si(100)



| 著者 | 庭野　道夫 |
| --- | --- |
| journal or publication title | Journal of Applied Physics |
| volume | 68 |
| number | 11 |
| page range | 5576-5583 |
| year | 1990 |
| URL | http://hdl.handle.net/10097/47807 |

doi: 10.1063/1.346993

# Synchrotron-radiation-induced decomposition of thin native oxide films on Si(100)

Michio Niwano, Hitoshi Katakura,[a] Yuji Takakuwa, and Nobuo Miyamoto
*Research Institute of Electrical Communication, Tohoku University, Sendai 980, Japan*

(Received 18 June 1990; accepted for publication 1 August 1990)

Thin native oxide films on Si(100) have been previously shown to be decomposed by exposing the film surface to synchrotron radiation (SR) in the vacuum-ultraviolet region. In this study, photoemission and photon-stimulated desorption (PSD) experiments are performed to investigate the synchrotron-radiation-induced decomposition of a native oxide film on Si(100). For mass analysis of the PSD ions, the time-of-flight method is utilized. Si 2*p* core-level and valence-band photoemission spectra demonstrate that the native-oxide decomposition preferentially takes place on the thin parts of the native oxide film which are terminated with Si--OH and Si--H bonds. It is shown that the native-oxide decomposition is accompanied by desorption of $H^+$ and $O^+$ ions. The $H^+$ PDS ion yield decreases exponentially with increasing the exposure time of SR, whereas the $O^+$ PSD one first increases with the exposure time, and subsequently decreases with the exposure time after the $H^+$ PSD ion yield substantially drops. The behavior of the $O^+$ PSD ion yield is explained in terms of the photon-induced Si--O bond breaking reaction promoted by removing surface hydrogen atoms through the $H^+$ PSD process in which a Si--H bond and the O--H bond in a Si--OH bond are ruptured.

## I. INTRODUCTION

An undesirable native oxide film formed by exposing a clean silicon surface to air, must be removed in the fabrication processings of metal-oxide-semiconductor (MOS) devices, e.g., silicon epitaxial growth, metallization, and thermal oxidation. In particular, this removal is quite important for generating an ultrathin gate oxide film by thermal oxidation methods, since native oxide remaining on a Si wafer surface is known to strongly influence the electrical and structural properties of a thin $SiO_2$ film grown on the surface. Up to now, removal of native oxide has usually been accomplished by heating the wafer at temperatures above about 800 °C. However, in order to fabricate high-reliable ultra-large-scale integration (ULSI) devices, it has become necessary to develop the low-temperature processing which does not rely on thermal activation methods. This is mainly because high-temperature treatment of Si wafers induces the formation of various types of defects which leads to degradation in the performance of ULSI devices. One efficient means to realize such a low-temperature processing is to utilize photon-excited process. Fortunately, with the recent development of synchrotron radiation (SR) sources, which provide a high level of radiation ranging from infrared to x ray, SR-excited processing is becoming a promising technique for the fabrication of electronic devices.[1-4]

In a previous paper,[5] we have revealed that a thin native oxide film on Si(100) is decomposed with the stimulating action of SR in the vacuum-ultraviolet (VUV) region (VUV-SR), suggesting that native oxide on a Si(100) wafer can be removed at low temperatures by exposing the wafer surface to VUV-SR. In this study, we perform photoemission and photon-stimulated desorption (PSD) experiments to understand how native oxide films on Si(100) are decomposed with VUV-SR. For mass analysis of the PSD ion products, we utilize the time-of-flight (TOF) method. From photoemission data, it is determined that the SR-induced decomposition of native oxide dominantly occurs on thin portions of the native oxide film. We find that the native-oxide decomposition is accompanied by desorption of $O^+$ and $H^+$ ions, and that the $H^+$ and the $O^+$ PSD ion yields exhibit a quite different behavior in the SR-exposure-time dependence. An explanation for the exposure-time dependence of the $O^+$ PSD ion yield is made.

## II. EXPERIMENT

Samples used were B-doped *p*-type Si(100) wafers with a resistivity of 10 Ω cm. The wafer surface was cleaned in the following manner: 15 min in boiling $NH_4OH:H_2O_2:H_2O$ (1:2:10) (RCA rinse), a deionized (DI) water rinse, $HF:H_2O$ (1:20) dip, DI rinse, 15 min in IPA vapor, and $N_2$ dry blow. Formation of native oxide on the wafer occurred predominantly after this surface cleaning while the wafer was being transferred to an ultrahigh vacuum (UHV) experimental chamber with facilities for photoemission spectroscopy. The base pressure of the chamber was below $1\times10^{-10}$ Torr.

Photoemission and PSD measurements were carried out at the Synchrotron Radiation Laboratory of the Institute of Solid State Physics, the University of Tokyo. SR emitted from a 0.4 GeV electron storage ring was used as

[a]Present address: Sony Magnetic Products Inc., Tagajyo-shi, Miyagi 985, Japan.



Downloaded 24 Mar 2010 to 130.34.135.83. Redistribution subject to AIP license or copyright; see http://jap.aip.org/jap/copyright.jsp

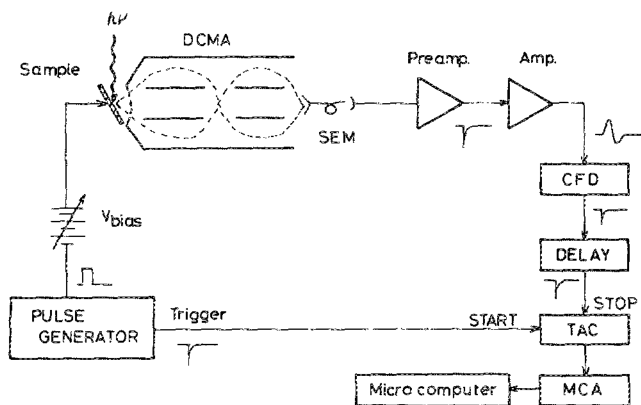


FIG. 1. Schematic diagram of the TOF measurement system used for mass analysis of PSD ions. DCMA double-pass cylindrical mirror analyzer, SEM secondary-electron multiplier, CFD constant-fraction discriminator, DELAY delay line, TAC time-to-amplitude converter, MCA multichannel analyzer.

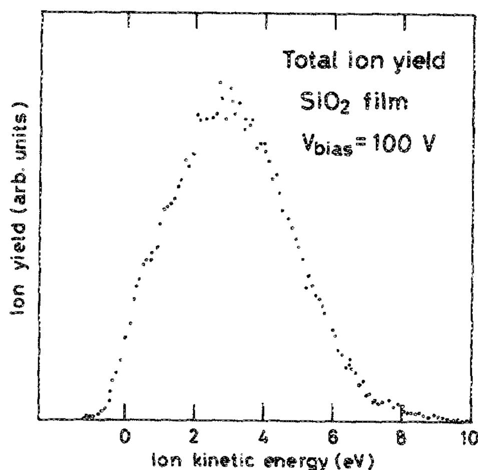


FIG. 2. Kinetic energy distribution of PSD ions from a thermally grown silicon oxide film.

a light source for these measurements. The critical energy of the radiation was 111 eV, with useful flux up to about 140 eV. For photoemission measurements, the radiation was monochromatized with a grazing-incidence monochromator which covers the photon energy range from 40 to 140 eV. For PSD measurements, the unmonochromatized zero-order ("white") SR emerging from the monochromator was used as a stimulating light source. The energy distribution curves of the "white" SR, which were obtained from measurements of the photoelectric yield of gold, exhibited a peak in photon flux at about 100 eV with a FWHM of about 50 eV. The total photon flux of this radiation was $10^{10}$–$10^{11}$ photons/s on the sample, and the spot size was within $1\times 1$ mm. Photoelectrons and PSD positively charged ions emitted from the sample surface were detected with a double-pass cylindrical mirror analyzer (DCMA). For detection of the PSD positive ions, the polarity of the voltage applied between the inner and outer cylindrical electrodes of the analyzer was reversed as compared to the case of photoelectron detection. This enabled us to perform both photoemission and PSD measurements without changing the experimental setup. Mass analysis of the PSD ions was carried out using the TOF method. An outline of the TOF measurement system used here has already been described previously.[5] We will present here a detailed account of the system.

Figure 1 shows a block diagram of the TOF measurement system. The flight time of a PSD ion passing through the analyzer, which is proportional to the square root of the ion mass, was measured with a time-to-amplitude converter (TAC), which provides an output pulse with an amplitude proportional to the time interval between a start input and a subsequent stop input. In general, the kinetic energy of PSD ions is rather low, typically a few electron volts.[6-8] In Fig. 2, we plot a kinetic energy distribution curve of PSD ions emitted from a 17-Å thick thermally-grown $SiO_2$ film on Si(100) during exposure of the film surface to the "white" SR as mentioned above. This curve has been measured with a positive potential of 100 V applied to the sample, as mentioned below. We see that the average kinetic energy of the PSD ions is about 3 eV. The transmittance of the DCMA for such a low-kinetic-energy ion is very low. Furthermore, we observed that the PSD ion signal level was rather low as compared to the photoelectron signal level. Thus, a positive potential of about 100 V was applied to the sample. Owing to the electric field generated between the sample and the grounded first grid of the DCMA, PSD ions emitted from the sample surface were efficiently collected by the analyzer and accelerated to about 100 eV kinetic energy. Accordingly, the pass energy of the analyzer was set at 105 eV, which should be compared to the pass energy of 20 eV as used in the photoemission measurements. This high pass energy enhanced the transmittance of the analyzer, which was also suited for detecting weak PSD ion signals. For measuring the ion flight times, a bias potential of about 85 V plus a pulsed potential of 15 V with a temporal width of 1 $\mu$s and a repetition rate of one pulse per 40 $\mu$s, the latter of which was synchronized with a start input pulse fed to the TAC, were applied to the sample as shown in Fig. 1. When only the bias potential was applied, no PSD ion could pass through the analyzer, since the kinetic energy of the ions, about 90 eV, was lower than the pass energy of the analyzer. When the pulsed potential was additionally applied to the sample, the PSD ions were accelerated to pass through the analyzer and reached the electron/ion detector, a secondary electron multiplier (SEM). A stop input pulse fed to the TAC was obtained from the ion detector. The pulse height of the TAC output was analyzed with a multichannel analyzer (MCA).

From a simple calculation we predict that for the pass energy of 105 eV, the flight time of an ion passing through the DCMA is 2.8 $\mu$s for $H^+$ and 11 $\mu$s for $O^+$, provided that the axial length of the analyzer is 30 cm and the acceptance angle of the analyzer is 42.3° with respect to the analyzer axis.



Downloaded 24 Mar 2010 to 130.34.135.83. Redistribution subject to AIP license or copyright; see http://jap.aip.org/jap/copyright.jsp

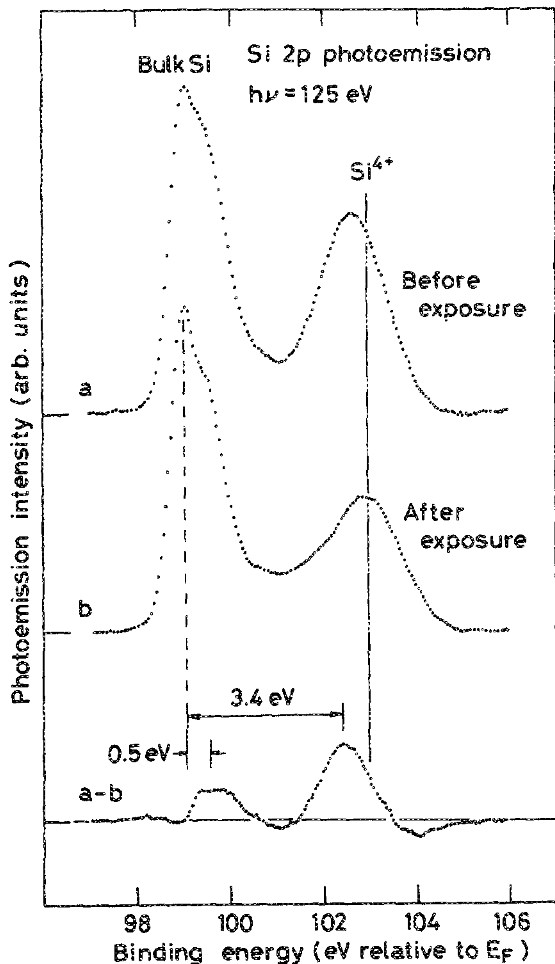


FIG. 3. Si $2p$ photoemission spectra of a native oxide film taken (a) before and (b) after SR exposure, and the difference between the two. A vertical solid line indicates the expected $Si^{4+}$ ($SiO_2$) energy position.

## III. RESULTS

### A. Si $2p$ core-level photoemission spectra

Figure 3 shows background-subtracted Si $2p$ core-level photoemission spectra of a native oxide film on Si(100) measured before and after 1 h exposure of the film surface to the "white" SR emerging from the monochromator. Two peaks are identified at binding energies of 99 and 103 eV. The 99 eV peak corresponds to photoemission of the Si $2p$ core-level electron mainly from Si atoms in the bulk Si crystal, and the 103 eV peak corresponds to that from Si atoms in the oxide film. It is seen from the figure that the oxide peak decreases in intensity after SR exposure. This change is due to a decrease in the oxide film thickness, indicating the occurrence of decomposition of the native oxide film due to VUV-SR exposure. In Fig. 3 we also show a difference between the two spectra, which represents changes in the surface chemical state caused by SR exposure. This difference spectrum displays two peaks shifted by 0.5 and 3.4 eV relative to the bulk Si peak. The 0.5-eV shifted peak can be interpreted as arising from photon-induced breaking of Si—H bonds existing on the substrate surface, because the Si $2p$ core-level chemical shift due to the bonding of a surface Si atom to hydrogen is reported to be about 0.3 eV.[9,10] Those Si—H bonds are considered to be predominantly generated during chemical cleaning of the wafer surface. The vertical solid line at 103 eV indicates the energy position at which the Si $2p$ core-level peak of amorphous $SiO_2$ ($Si^{4+}$) is expected to show up.[11] It should be noticed that the 3.4-eV shifted peak, which represents the decomposition of native oxide, is located by 0.5 eV lower than this expected $Si^{4+}$ position. Here we note that, as pointed out by Himpsel *et al.*[11] the Si $2p$ core-level of $SiO_2$ moves towards lower binding energies for films thinner than 5 Å due to a smaller valence band offset and extra screening by the Si substrate. Indeed, we confirmed that an 8-Å thick native oxide film has the oxide peak at the expected energy position. Furthermore, it is likely that during natural oxidation of a Si wafer an inhomogeneous oxide film is formed on the wafer surface., that is, thin and thick oxide overlayers coexist on the surface. We therefore interpret that the decomposed component of native oxide, which corresponds to the 3.4-eV shifted peak in the difference spectrum, initially resided on thin portions of the native oxide film. On the other hand, the oxide peak after SR exposure, which is located at the expected $Si^{4+}$ position, can be explained as arising from thick portions of the oxide film. We observed that this oxide peak does not exhibit any substantial change with further exposure to the SR. Hence, we conclude that the SR-induced decomposition of a native oxide film on Si(100) preferentially takes place on thinner portions of the oxide film, while thicker portions of the oxide film do not change upon VUV-SR exposure.

It is well established that at the $SiO_2$/Si interfacial region, there exist Si atoms in intermediate oxidation states, i.e., $Si^{1+}$ ($Si_2O$), $Si^{2+}$ (SiO), and $Si^{3+}$ ($Si_2O_3$), which correspond to the interfacial Si atoms which are bonded to one, two, and three oxygen atoms, respectively.[12–14] These intermediate oxidation states, which are called "suboxide", appear as a separated peak between the bulk Si and the oxide peaks in Si $2p$ core-level spectra due to different Si $2p$ core-level chemical shifts.[11] We expected that during SR exposure suboxides at the $SiO_2$/Si interface change in the density with decomposition of the overlying native oxide film. We have therefore performed a detailed analysis of the Si $2p$ core-level spectra as presented in Fig. 3, to examine the effects on the suboxide density due to SR exposure.

In analyzing the Si $2p$ core-level spectra, we have taken account of Si atoms in the following bonding states, which give rise to different chemical shifts of the Si $2p$ core level. First, suboxides $Si^{n+}$ ($n = 1,2,3$) as mentioned above were taken into account in the analysis. Second, on the basis of the above argument, we considered two kinds of Si atoms in the native oxide film; one corresponds to thinner portions of the native oxide film, and the other to thicker portions of the oxide film. It was assumed that the former, to which we will refer as $SiO_2^*$ here, provides a Si $2p$ core-level peak located slightly lower than expected $Si^{4+}$ ($SiO_2$) energy position, whereas the latter provides a Si $2p$ core-level peak at the expected $Si^{4+}$ position. We also



Downloaded 24 Mar 2010 to 130.34.135.83. Redistribution subject to AIP license or copyright; see http://jap.aip.org/jap/copyright.jsp

TABLE I. Energy position and intensity for each component.

| | Energy[a] (eV) | Intensity[b] | |
|---|---|---|---|
| | | Before SR exposure | After SR exposure |
| Si − H | 0.35 | 0.41 | 0.19 |
| $Si^{1+}$ | 1.0 | 0.32 | 0.21 |
| $Si^{2+}$ | 1.8 | 0.13 | 0.09 |
| $Si^{3+}$ | 2.5 | 0.17 | 0.17 |
| $SiO_2^*$ | 3.2 | 0.42 | 0.14 |
| $SiO_2(Si^{4+})$ | 3.9 | 0.86 | 0.68 |

[a]Relative to the energy position of the bulk Si component.
[b]Relative to the intensity of the bulk Si component.

considered such a surface Si atom that is bonded to hydrogen. The presence of this bonding state is evident from the difference spectrum shown in Fig. 3, which exhibits a peak arising from ruptured Si—H bonds. Hence, using a least-squares fitting procedure, we have decomposed the Si $2p$ core-level photoemission spectra into seven components, i.e., bulk Si, Si—H, $Si^{n+}$ $(n = 1,2,3)$, $SiO_2^*$, and $SiO_2$ $(Si^{4+})$, with each component having voigt shape, i.e., a Lorentzian convoluted with a Gaussian. The peak width for each component consists of the contributions due to the instrumental energy resolution, the inhomogeneous broadening, and the lifetime broadening. The overall instrumental energy resolution was 0.43 eV in the present measurement system. The lifetime broadening was taken into account by a Lorentzian of 0.1 eV FWHM. The inhomogeneous broadening is related to the degrees of structural freedom and increases as the number of Si—O bonds around a given Si atom increases. The Gaussian FWHMs due to this broadening for suboxides and $Si^{4+}$ were the same as given by Himpsel *et al.*[11] and those for Si—H and $SiO_2^*$ were assumed to be the same as for the bulk Si and $Si^{3+}$, respectively. The energy position for each component used to fit the Si $2p$ core-level spectra is tabulated in Table I. The energy positions for suboxides and $Si^{4+}$ $(SiO_2)$ were almost the same as given by Himpsel *et al.*[11] The spectra have also been decomposed into the Si $2p_{3/2}$ and Si $2p_{1/2}$ spin-orbit partner lines. For this decomposition, the spin-orbit splitting of 0.61 eV and the $2p_{1/2}$ and $2p_{3/2}$ intensity ratio of 1:2 were assumed.

The results of the analysis are summarized in Fig. 4 and Table I. In Fig. 4, only the Si $2p_{3/2}$ photoemission lines normalized in intensity to the intensity of the bulk Si peak are shown. Agreement between the experimental and the calculated spectral curves is fairly good. We can see from Fig. 4 and Table I that components Si—H and $SiO_2^*$ remarkably decreased in intensity after SR exposure. This confirms that SR exposure caused breaking of Si—H bonds on the Si substrate and decomposition of thin portions of the native oxide film. On the other hand, the suboxide intensities did not decrease drastically after SR exposure. The reason for this would be that the suboxides existing at the interface between the Si substrate and the undecomposed thick native oxide overlayer, have remained after SR exposure. Nevertheless, a decrease in the intensities of $Si^{1+}$ and $Si^{2+}$ is identified. Here we will consider the origin of the suboxides $Si^{1+}$ and $Si^{2+}$. One possible origin of a $Si^{2+}$ state is the silicon atom at the $SiO_2$/Si(100) interface which is bonded to two oxygen atoms (see Fig. 9). The bonding of a surface Si atom on the Si(100) substrate to two oxygen atoms also gives rise to a $Si^{2+}$ state. Alternatively, when one of the two unsaturated bonds of a surface Si atom on Si(100) is bonded to oxygen to generate a Si—OH bond and the other is bonded to hydrogen, the Si atom corresponds to a $Si^{1+}$ oxidation state, It is most likely that, together with surface Si—H bonds mentioned previously, Si—OH bonds which are probably generated during chemical cleaning of the wafer surface, partially cover a naturally oxidized Si(100) surface. Thus, we can interpret the observed decrease in intensity of $Si^{1+}$ and $Si^{2+}$ as due to rupture of Si—OH bonds on the substrate surface as well as decomposition of the native oxide overlayer.

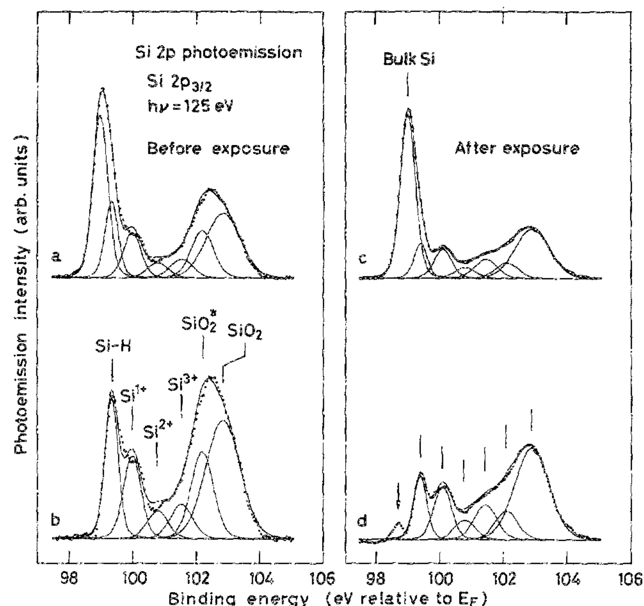


FIG. 4. Si $2p_{3/2}$ photoemission spectra (a) before and (c) after SR exposure. Dots are the measured data and the solid line is the result of a least-squares fit. The spectra (b) and (d) as shown on enlarged scales have been obtained by subtracting the bulk Si component from the spectra (a) and (c), respectively.

It is interesting to notice that there appears an additional peak on the low-energy side of the Si—H peak in the spectrum after SR exposure, as shown in Fig. 4(d). The peak, which is indicated by an arrow in the figure, is shifted by about 0.3 eV to lower binding energies relative to the bulk Si peak. We attribute this peak to surface Si atoms with unsaturated dangling bonds, because the Si $2p$ core-level chemical shift for those silicon atoms is 0.43 eV relative to the bulk Si peak.[9] The appearance of this surface silicon peak after SR exposure, indicates that the clean surface has appeared due to the exposure of the naturally oxidized Si(100) surface to VUV-SR.



Downloaded 24 Mar 2010 to 130.34.135.83. Redistribution subject to AIP license or copyright; see http://jap.aip.org/jap/copyright.jsp

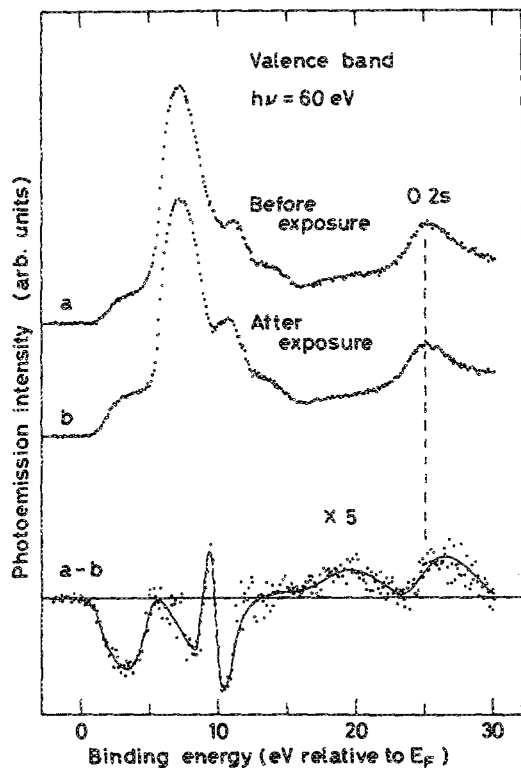


FIG. 5. Valence band photoemission spectra (a) before and (b) after SR exposure, and the difference between the two.

### B. Valence-band photoemission spectra

In Fig. 5 we present valence-band photoemission spectra of the native oxide film taken before and after 1 h exposure of the white VUV-SR. These spectra have been normalized in intensity to the number of incident photons. A shoulder appearing at a binding energy of 3 eV is due to photoemission from the bulk Si valence band of 3*p* character. We note that this shoulder decreases in intensity with increasing oxide film thickness due to attenuation by the $SiO_2$ overlayer.[12] A pronounced peak at 7 eV and weak peaks at 12 and 14 eV are attributed to photoemission from the $SiO_2$ valence band of O 2*p* character. A peak appearing at 25 eV arises from photoemission of the O 2*s* shallow core-level electron. In Fig. 5, the difference between the two spectra is also plotted on an enlarged scale. Looking at this difference spectrum, we see that the shoulder at 3 eV increased in intensity after SR exposure, suggesting a decrease in the oxide film thickness due to SR exposure. In addition, the O 2*s* peak decreased in intensity after SR exposure, indicating a decrease in the surface oxygen concentration, that is, desorption of oxygen atoms from the naturally oxidized Si surface due to SR exposure. These results support the conclusion derived from the results of Si 2*p* core-level photoemission measurements that a native oxide film on Si(100) is decomposed with the stimulating action of VUV-SR.

We notice that the peak at 26 eV in the difference spectrum, which indicates desorption of oxygen atoms from the naturally-oxidized Si(100) surface, is slightly shifted to higher binding energies relative to the O 2*s* peak position as indicated by a dashed line in the figure. This energy shift provides a clue as to the origin of the oxygen atoms desorbed. It is known that below about 450 K, water adsorbs on a Si(100) surface with an unusually high sticking coefficient near unity.[15] Chabal and Christman[16] interpreted this adsorption as partly dissociated water, that is, formation of Si—OH and Si—H bonds on the substrate surface. The photoemission studies of Ranke and Xing[15] have demonstrated that the O 2*s* photoemission line is positioned by about 0.5 eV higher binding energy for the $H_2O$-exposed Si(100) surface than for the well-oxidized silicon surface which favors the bridge bond configuration Si-O-Si for the adsorbed oxygen.[15,17] From these facts, we deduce that the desorbed oxygen atoms originates dominantly from Si—OH bonds on the naturally oxidized Si(100) surface.

As can be seen from the difference spectrum in Fig. 5, there is an apparent discrepancy in spectral shape between the spectra before and after SR exposure, in the energy region from 5 to 12 eV where the $SiO_2$-related peaks show up. One possible origin of this discrepancy is the decomposition of thin portions of the native oxide film. However, there is another possibility that a change in the electronic structure of the undecomposed thick native oxide films caused by SR exposure is responsible for the discrepancy. Which mechanism dominates is not clear at present.

### C. TOF mass spectra

Figure 6 shows TOF mass spectra of PSD ions emitted from the native oxide and thermally grown oxide films during exposure of the film surfaces to the "white" SR emerging from the monochromator. These spectra have been taken immediately after the beginning of SR exposure and normalized in ion yield to the number of incident photons. A time scale is attached to the figure. The origin of the flight time was set at the position where a photoelectron TOF peak appeared, because an electron has a mass considerably smaller than ions and thus its flight time is negligible. As shown in Fig. 6(a), two peaks at flight times of 3 and about 12 $\mu$s are identified on the native oxide film. From the prediction mentioned in the previous section, we determine that the pronounced peak at 3 $\mu$s is due to desorption of $H^+$ ions and the peak at 12 $\mu$s to that of $O^+$ ions. Here we cannot rule out the possibility that $OH^+$, which could be resolved from $O^+$ ion signals in the present TOF measurement system, is another origin of the peak at 12 $\mu$s. Furthermore, there also exists the possibility of $F^+$ partly contributing the peak of concern. However, we believe that in the present case, the $F^+$ contribution is rather small as compared to the $O^+$ and $OH^+$ ones, since no F 2*s* core-level line was observed in valence-band photoemission spectra of the naturally-oxidized Si surface investigated here. For simplicity, therefore, we shall refer to the peak at 12 s as the $O^+$ peak here. The $O^+$ PSD can be naively interpreted as arising from the decomposition of native oxide, as described previously.[5] The $H^+$ PSD is regarded as due to rupture of a Si—H bond and that of the O—H bond in a Si—OH complex. Comparing the mass spectrum of the native oxide film with those of the



Downloaded 24 Mar 2010 to 130.34.135.83. Redistribution subject to AIP license or copyright; see http://jap.aip.org/jap/copyright.jsp

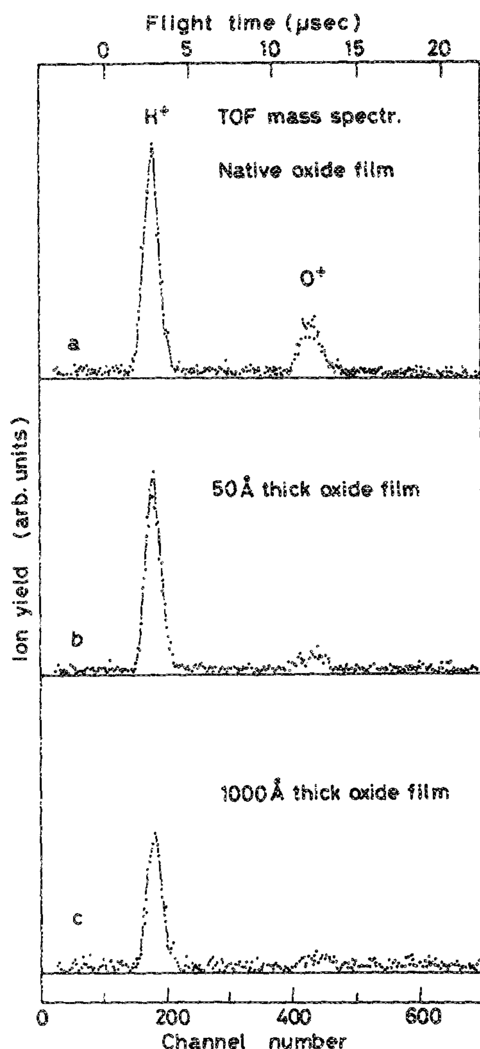


FIG. 6. TOF mass spectra of PSD ions from (a) a native oxide film exposed to SR, compared with those from (b) 50-Å and (c) 1000-Å-thick thermally grown silicon oxide films exposed to SR.

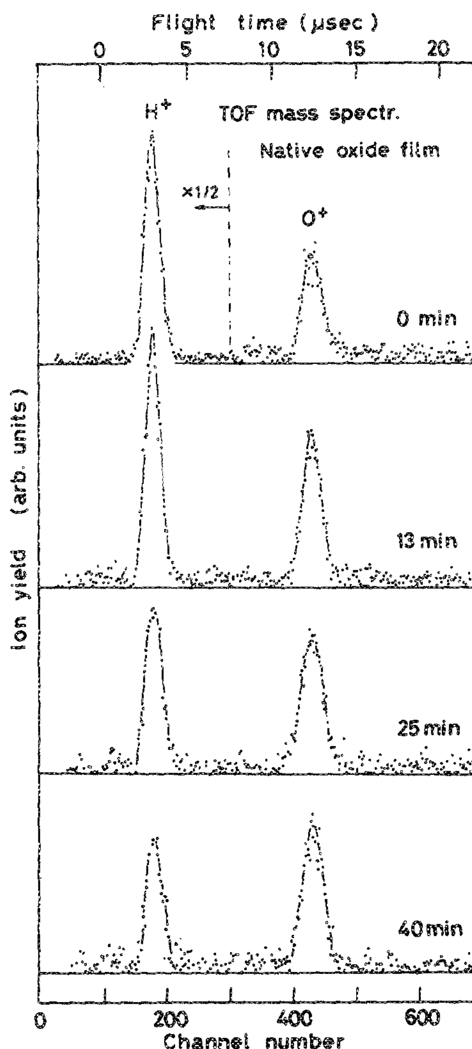


FIG. 7. TOF mass spectra of a native oxide film taken at different exposure times of SR.

thermally-grown oxide films as shown in Figs. 6(b) and 6(c), we see that the native oxide film exhibits relatively large $O^+$ PSD ion signals as compared to the thermally grown oxide films. This strongly suggests that native oxide films are more easily decomposed with VUV-SR than thermally grown oxide films.

In Fig. 7, we show TOF mass spectra of the native oxide film taken at different exposure times of SR. The ion yield has been normalized to the number of incident photons. The $H^+$ PSD peak drastically decreases in intensity with increasing the exposure time. For clarity, we have plotted the peak areas for $H^+$ and $O^+$ as a function of the exposure time of SR in Fig. 8. The $H^+$ PSD ion yield exhibits an exponential decrease with the exposure time. In our previous works, we observed large $H^+$ PSD ion signals on the oxygen-exposed silicon surfaces[18] and the HF-treated silicon surface[19] during exposure of the surfaces to VUV-SR. It appears that hydrogen easily desorbs from a silicon surface with the stimulating action of VUV-SR. The exponential decrease in the $H^+$ PSD ion yield therefore means that hydrogen atoms existing on the naturally oxidized Si surface has been driven out via the $H^+$ PSD process during a relatively short term of SR exposure. On the other hand, the $O^+$ ion yield exhibits a quite different behavior; it first increases with the exposure time of SR, saturates when the $H^+$ ion yield substantially drops, and subsequently decreases. This behavior of the $O^+$ PSD ion yield will be discussed in the following section.

## IV. DISCUSSION

Our experimental results demonstrate that thin native oxide films are readily decomposed with VUV-SR as compared to thick native oxide films or thermally grown oxide ones. In order to understand why this occurs, we first discuss the atomic bonding configuration of the native oxide film investigated here.

Previous studies revealed that water readily adsorbs on a Si(100) surface to generate Si—OH and Si—H,[15,16] and also that water contained in the atmosphere plays a crucial role in the formation of native oxide on Si wafers.[20] Under



Downloaded 24 Mar 2010 to 130.34.135.83. Redistribution subject to AIP license or copyright; see http://jap.aip.org/jap/copyright.jsp

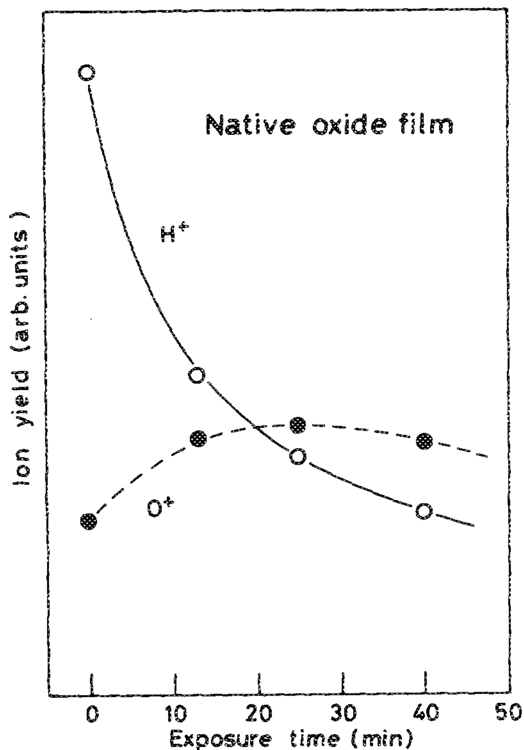


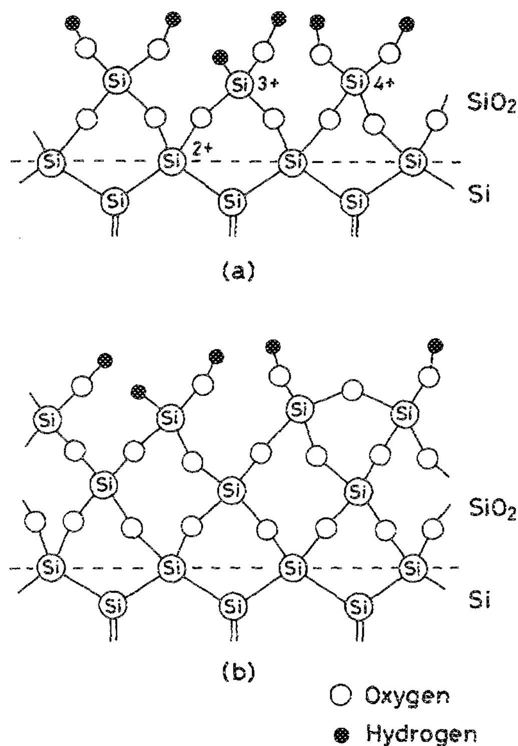


FIG. 8. Dependence of the $H^+$ and $O^+$ ion yields on the exposure time of SR.

FIG. 9. Schematic of the atomic configurations for (a) thin and (b) thick portions of a native oxide film on Si(100).

these circumstances, we can expect that the surface of a native oxide film on Si(100) is dominantly terminated with Si—OH and Si—H bonds. In other words, we may say that a native oxide film surface is terminated with hydrogen. Furthermore, it would be reasonable to assume that the thin portions of our native oxide film which were decomposed with VUV-SR, are one oxide monolayer in thickness, about 5 Å thick, at the most. This is because the average thickness of those portions, which was obtained from the relative photoemission intensity of $SiO_2^*$ as listed in Table I using Eq. (3a) in Ref. 11, is only 1.5 Å before SR exposure. Thus, we suggest a model of atomic configuration for the thin portions of the native oxide film as schematically illustrated in Fig. 9(a). The thickness of thick portions of the native oxide film, on the other hand, will be two oxide monolayers or more. One plausible atomic configuration expected for those portions is shown in Fig. 9(b).

Now we will consider the reason why a thin native oxide film about one monolayer thick is more easily decomposed with VUV-SR than thicker native oxide or thermally grown oxide films. An important point in interpreting this phenomenon is the difference in the atomic bonding configuration among these oxide films. A thermally grown oxide film is considered to be mainly consisted of the Si—O—Si bridge bond. This would also be the case for thick native oxide films, although the surface is partly terminated with Si—OH and Si—H bonds, as shown in Fig. 9(b). On the other hand, a thin native oxide film with one monolayer thick is terminated with Si—OH and Si—H bonds, and moreover, it has a smaller number of Si—O—Si bonds, as shown in Fig. 9(a). Here we expect that it is much hard for breaking of the Si—O—Si bridge bond to occur under irradiation of VUV-SR, because the oxygen atom in this bond is bonded to two neighboring silicon atoms. This is consistent with the experimental result that thermally grown oxide and thick native oxide films, which mainly consist of the Si—O—Si bridge bond, were not easily decomposed with VUV-SR. On the other hand, Si—OH and Si—H bonds will be more easily broken with VUV-SR than the Si—O—Si bridge bond. This is because there observed large $H^+$ PSD signals arising from rupture of a Si—H bond and that of the O—H bond in a Si—OH bond, and the oxygen atom in an Si—OH bond is bonded to only one Si atom. Thus, we interpret that Si—OH and Si—H bonds on thin portions of a native oxide film are readily broken with VUV-SR, thereby leading to decomposition of those portions. However, it is expected that Si—O—Si bridge bonds in thin native oxide films are not completely broken with VUV-SR, and Si—O bonds are, as a result, partly left behind on the substrate surface after SR exposure. This would be another reason why the suboxide intensities did not remarkably decrease after SR exposure. Si—OH and Si—H bonds existing on the substrate surface will be almost completely broken with VUV-SR. We think that this surface bond breaking reaction, together with the decomposition of thin native oxide films, gives rise to the clean silicon surface.

Finally, we discuss the observed dependence of the $O^+$ PSD ion yield on the exposure time of SR. As mentioned above, we interpreted that the decomposition of thin



Downloaded 24 Mar 2010 to 130.34.135.83. Redistribution subject to AIP license or copyright; see http://jap.aip.org/jap/copyright.jsp

native oxide films proceeds through the breaking of surface Si—OH and Si—H bonds. Here we assume that the decomposition of a native oxide film, which gives rise to desorption of $O^+$ ions, is enhanced by removing hydrogen atoms adsorbed onto the oxide film surface. That is, when the surface hydrogen atoms are driven out via the $H^+$ PSD process, in which breaking of a Si—H bond and that of the O—H bond in a Si—OH bond would occur, it becomes easy for subsequent breaking of the remaining Si—O bonds to occur. This could explain why the $O^+$ PSD ion yield first increased with increasing the exposure time of SR. Once a substantial part of the surface hydrogen atoms are taken away, the remaining oxygen atoms bonded to Si atoms in native oxide will successively desorb via the $O^+$ PSD process. This would be the reason why the $O^+$ ion yield decreased gradually with the exposure time of SR, after the $H^+$ ion yield substantially dropped. Of course, we expect that a direct breaking of the Si—O bond in a Si—OH complex, which induces desorption of $OH^+$ ions, also occurs. This breaking reaction explains the $O^+$ ion yield observed at the beginning of SR exposure.

## V. CONCLUSIONS

The sychrotron-radiation-induced decomposition of native oxide on Si(100) has been studied using photoemission and PSD spectroscopic techniques with SR. The results of Si $2p$ core-level and valence-band photoemission measurements demonstrate that the decomposition of native oxide preferentially occurs on the thin portions of a native oxide film on Si(100) which are terminated with Si—OH and Si—H bonds. It was shown that the native-oxide decomposition is accompanied by desorption of $H^+$ and $O^+$ ions. The $O^+$ and $H^+$ PSD yields display a quite different behavior in the SR-exposure time dependence; the $O^+$ ion yield first increases and subsequently decreases with increasing the exposure time of SR, whereas the $H^+$ ion yield exponentially decreases with the exposure time. The behavior of the $O^+$ PSD ion yield was qualitatively explained in terms of the photon-induced Si—O bond breaking reaction promoted by the removal of hydrogen atoms adsorbed onto a native oxide film surface via the $H^+$ PSD process.

## ACKNOWLEDGMENTS

The authors wish to thank Dr. K. Yagi and Dr. A. Hiraiwa of the Central Research Laboratory, Hitachi Ltd., for sample preparation. The excellent support of the staff of the Synchrotron Radiation Laboratory of the Institute for Solid State Physics, the University of Tokyo, is gratefully acknowledged.

[1] H. Kuragi and T. Urisu, Appl. Phys. Lett. **50**, 1254 (1987).
[2] H. Kuragi and T. Urisu, J. Appl. Phys. **61**, 2035 (1987).
[3] F. Cerrina, B. Lai, G. M. Wells, J. R. Wiley, D. G. Kilday, and G. Margaritondo, Appl. Phys. Lett. **50**, 533 (1987).
[4] R. Zanoni, M. N. Piancastelli, J. McKinley, and G. Margaritondo, Appl. Phys. Lett. **55**, 1020 (1989).
[5] M. Niwano, H. Katakura, Y. Takakuwa, N. Miyamoto, A. Hiraiwa, and K. Yagi, Appl. Phys. Lett. **56**, 1125 (1990).
[6] D. M. Hanson, R. Stockbauer, and T. E. Madey, Phys. Rev. B **24**, 5513 (1981).
[7] J. F. van der Veen, F. J. Himpsel, D. E. Eastman, and P. Heimann, Solid State Commun. **36**, 99 (1980).
[8] E. D. Johnson, R. F. Garrett, M. L. Knotek, and F. Sette, in *Desorption Induced by Electronic Transitions, DIET III*, edited by R. H. Stulen and M. L. Knotek (Springer, Berlin, 1988), p. 210.
[9] C. U. S. Larsson, A. S. Flodström, R. Nyholm, L. Incoccia, and F. Senf, J. Vac. Sci. Technol. A **5**, 3321 (1987).
[10] C. J. Karlsson, E. Landemark, L. S. O. Johansson, U. O. Karlsson, and R. I. G. Uhrberg, Phys. Rev. B **41**, 1521 (1990).
[11] F. J. Himpsel, F. R. McFeely, A. Taleb-Ibrahimi, J. A. Yarmoff, and G. Hollinger, Phys. Rev. B **38**, 6084 (1988).
[12] G. Hollinger and F. J. Himpsel, J. Vac. Sci. Technol. A **1**, 640 (1983).
[13] G. Hollinger and F. J. Himpsel, Appl. Phys. Lett. **44**, 93 (1984).
[14] P. J. Grunthaner, M. H. Hecht, F. J. Grunthaner, and N. M. Johnson, J. Appl. Phys. **61**, 629 (1986).
[15] W. Ranke and Y. R. Xing, Surf. Sci. **157**, 339 (1985).
[16] Y. J. Chabal and S. B. Christman, Phys. Rev. B **29**, 6974 (1984).
[17] W. Ranke and Y. R. Xing, Surf. Sci. **157**, 353 (1985).
[18] Y. Takakuwa, M. Niwano, M. Nogawa, H. Katakura, S. Matsuyoshi, H. Ishida, H. Kato, and N. Miyamoto, Jpn. J. Appl. Phys. **28**, 2581 (1989).
[19] Y. Takakuwa, M. Nogawa, M. Niwano, H. Katakura, S. Matsuyoshi, H. Ishida, H. Kato, and N. Miyamoto, Jpn. J. Appl. Phys. **28**, L1274 (1989).
[20] M. Morita, T. Ohmi, E. Hasegawa, M. Kawakami, and K. Suma, Appl. Phys. Lett. **55**, 562 (1989).



Downloaded 24 Mar 2010 to 130.34.135.83. Redistribution subject to AIP license or copyright; see http://jap.aip.org/jap/copyright.jsp